DOPPLER-BASED ULTRASONIC BLOOD VELOCITY ESTIMATION

BY

TOROS ARIKAN

THESIS

Submitted in partial fulfillment of the requirements
for the degree of Bachelor of Science in Electrical and Computer Engineering
in the Undergraduate College of the
University of Illinois at Urbana-Champaign, Fall 2014

Urbana, Illinois

Adviser:

Professor Andrew C. Singer

Abstract

Blood velocity estimation is a useful clinical tool for assessing the condition of blood vessels and organ functionality. Current methods monitor the shift of position of red blood cells over time to estimate velocity, and generally do not use Doppler shift information. The tracking of these particles based on their shifts in position is a computationally intensive and time-consuming process. The development of Doppler-based methods using short chirps would allow significantly faster calculations because the positions of particulates would not have to be tracked over several pulses. Use of additional information embedded in the received waveform would also allow operation in a noisier environment. We investigate the feasibility of such a system for linear, hyperbolic and superposed hyperbolic chirps. Interrogation of a simulated blood vessel with these chirps, followed by correlation with a filter bank, demonstrates the chirps' Doppler insensitivity for the given constraints. The true ambiguity functions of the chirps are plotted, and short signal duration is found to be the cause of the small Doppler resolution we obtain. Cramér-Rao lower bounds in Doppler are calculated for the case of a simple delayed and Doppler-shifted chirp, and the results indicate that a Doppler-based approach is feasible. Future research will refine the Cramér-Rao lower bound to incorporate attenuation and other physical effects, which will increase the SNR we need to obtain a given Doppler resolution, We will also focus on modifying the chirps used to interrogate blood vessels to have greater Doppler resolution.

Keywords: Ultrasound, Doppler, Cramér-Rao Lower Bound, Blood Velocity, Signal Processing

Contents

1. Introduction

Real-time blood flow measurement is an important biomedical application in ultrasonic imaging, useful in assessing the condition of blood vessels and organ functionality. Real-time vector map estimates of blood flow in the body obtained with ultrasound are currently used for fast clinical diagnosis of vascular disorders. This form of blood flow measurement has great clinical value over invasive procedures, but is difficult to perform accurately for a number of reasons. Pulses of ultrasound used to measure blood flow need to have short durations for real-time imaging, and the bandwidth of the pulse is constrained by the capabilities of biomedical devices. Blood flow is also slow compared to the propagation speed of ultrasound through the body. These factors make it difficult to accurately estimate Doppler from a blood vessel. In addition to these natural constraints, there are also practical difficulties in positioning a transducer at the correct angle to obtain the best Doppler estimate [1]. The majority of current methods estimate the rate of change of phase of a returning signal, or monitor the shift in position of red blood cells through their scattering signature, to determine blood flow velocity. Neither approach makes use of Doppler information [2]. The limitations of classical Doppler-shift methods are the result of limited Doppler resolution due to problem constraints, in addition to frequency-dependent attenuation and scattering in the body [3]. However, if Doppler shift information could be successfully acquired from the received waveform, we could obtain velocity estimates with only a few chirps, because we would no longer have to track particulates. This would allow significantly faster calculations, with only several short chirps needed to obtain results. While the literature discourages the use of a Doppler-based technique, these studies were conducted several decades ago, and it is possible that recent advances in signal processing and in computing capability can make Doppler methods practical.

Chapter 2 briefly reviews important literature on blood velocity estimation. Chapter 3 details the work performed to investigate the feasibility of a Doppler-based approach. Specifically, Section 3.1 defines the chirp signals and constraints used throughout the report; Section 3.2 gives the simulation results for a basic correlation method; Section 3.3 presents the ambiguity functions for the chirp signals; and Section 3.4 details the calculation of the Cramér-Rao Lower Bounds of the chirp signals, which indicate that our method is feasible. Chapter 4 concludes the report and presents our future work.

2. Literature Review

There are several comprehensive studies on blood velocity estimation. *Estimation of Blood Velocities Using Ultrasound* by Jørgen Arendt Jensen [3] details the basics of the signal processing work required, as well as the setup of the apparatus for the actual measurements. Jensen emphasizes the fact that, although blood velocity estimation systems are commonly called "Doppler ultrasound scanners," the majority of these do not use Doppler-shift information and instead estimate the rate of change of phase of a signal, or track the position of a defined group of scatterers through their scattering signatures. In the more recent review, "Ultrasonic colour Doppler imaging," by Evans, Jensen and Nielsen [2], current methods for blood velocity measurement are summarized and some open research problems are highlighted. There are two key areas of recent research: signal processing methods for velocity estimation, and the physical measurement methods used to obtain data, concerning the angle and placement of transducers. The review heavily references a 1985 paper by Chihiro Kasai, Koroku Namekawa, Akira Koyano, and Ryozo Omoto, "Real-Time Two-Dimensional Blood Flow Imaging Using an Autocorrelation Technique" [4]. This paper details a common procedure for blood velocity estimation, although improvements have been made since its publication. The paper is relevant to our research due to the procedure's similarity to our initial matched filter approach.

Unlike the method we are investigating, involving transmission of hyperbolic chirps and performing cross-correlation on the received reflected signal, current methods generally transmit a basic sine wave. The phase shifts or time delays between echoes from the same sample volume during subsequent pulses are monitored. Mean blood flow velocity is estimated from the frequency spectra of the echoes, by first calculating the mean Doppler frequency shift, and then using the approximation

$$v = \frac{\overline{\omega}}{\omega_0}\frac{c}{2\cos\theta}$$

where θ is the angle between the ultrasound beam and the blood flow vector, $\overline{\omega}$ is the mean angular frequency of the power spectrum of the complex envelope of the received signal, ω_0 is the carrier frequency and c is the ultrasound velocity. Kasai's paper details a number of approximations for calculating the mean Doppler frequency shift using an autocorrelation technique; but since we have much greater computation power, we could just perform the autocorrelation without modifications.

Extant CFI (color flow imaging) methods require 8-16 pulses to estimate the component of velocity towards the transducer, due to the stochastic nature of echoes from blood and the need to filter echoes from solid targets which generate interference of much higher amplitude than the desired signal. Clutter can exceed the blood velocity signal by 40-60 dB. Current methods are limited in their maximum frequencies because phase shifts between frames become too small to be reliably estimated when significantly oversampled. This means that filter design for filtering out background noise is challenging. Traditional FIR and IIR filtering approaches and simple echo cancelling do not perform well due to the limited number of samples in the case of FIR, long transient responses in the case of IIR, and poor cutoffs for echo cancellation. Increasing the frame rate by a different method would yield significant improvement in the performance of CFI systems.

A second CFI technique that is not as common as phase shift estimation is to measure changes in the round-trip time from a group of scatterers, identified by their scattering signature. Cross-correlation with similar segments of previous pulses allows identification how much the group of scatterers has moved spatially, allowing estimation of their velocity. There are some obvious issues with this method: the group of scatterers disperses over time, and significant differences may be observed between frames.

The most important problem studied in CFI research is three-dimensional blood flow velocity estimation and the superposition of vectors on blood flow in order to make clinical diagnosis much easier. The major considerations studied in the problem are the placement of transducers and different approaches to beamforming. A second significant problem tied to the first is to increase the frame rate for CFI so that blood vortices in the heart and other transient phenomena can be observed. Jensen states that pulsed-wave Doppler systems do not use the Doppler shift frequency of individual pulses, because frequency-dependent attenuation and frequency-dependent scattering drastically change the spectrum of the pulse. If we were able to estimate the Doppler shift in two short pulses, we would obtain a better frame rate that would allow us to better observe transient phenomena.

3. Description of Research Results

3.1 Chirp Definitions and Simulation Constraints

We use linear, hyperbolic and superposed hyperbolic chirp signals in our simulations. There are many expressions for these signals in the literature; for our purposes, a linear chirp is given by

$$C(t)_{linear} = Ae^{j2\pi(f_0 t + k_0 t^2/2)} \tag{3.1}$$

where f_0 is the initial frequency, A is an envelope for the transmitted signal, t is time in the range $[0,T]$ where T is the duration of the chirp, and k_0 is a constant determined for a given starting frequency, end frequency and signal duration as follows:

$$k_0 = \frac{f_{final} - f_0}{T} \tag{3.2}$$

For the hyperbolic chirp, we have the expressions

$$C(t)_{hyper} = Ae^{j(2\pi/k_0)\log(1+k_0 f_0 t)} \tag{3.3}$$

$$k_0 = \frac{1}{T}\left(\frac{1}{f_{final}} + \frac{1}{f_0}\right) \tag{3.4}$$

The instantaneous frequency of the chirp is given by the derivative of the phase term,

$$f(t) = \frac{1}{\frac{1}{f_0} + k_0 t} \tag{3.5}$$

yielding a hyperbolic expression with respect to time [5]. Note that the final frequency can be larger or smaller than the initial frequency f_0, yielding an up-chirp or a down-chirp. The superposed hyperbolic chirp is simply the sum of two hyperbolic up- and down-chirps with the same time duration and frequency range. The reason we wish to investigate the superposed chirp is that by cross-correlating the received waveform with an up-chirp and a down-chirp, and observing how the location of peak correlation changes, we hope to develop a method that does not rely on the common yet resource-intensive filter bank approach used in Section 3.2.

The two key variables analyzed in our research are delay and Doppler for a received signal. A signal reflected off a target acquires a time delay d given by the round-trip travel distance divided by the speed of propagation c. If the target is also moving relative to the observer, the signal reflected off the target will acquire a change in its frequency, called a Doppler shift. If the target is moving towards the source, the Doppler shift will be positive and the received wave will have a higher frequency; conversely, if the target is moving away from the source, the Doppler shift will be negative and the received wave will have a lower frequency. In the time domain, these shifts correspond to a compression and a stretch respectively. A target moving at velocity v with zero acceleration has stretch factor s, defined as

$$s = 1 - \frac{2v}{c} \tag{3.6}$$

When a signal undergoes a Doppler shift, it is stretched by s. It is easier for our purposes to work with this stretch factor rather than with the Doppler shift, because we work with expressions in the time domain rather than in the frequency domain. Notice that for a stationary target, there is zero Doppler and the stretch factor is 1.

In our simulations of blood velocity, we assume that the speed of propagation of ultrasound is fixed at c = 1570 m/s. Unless stated otherwise, the chirp duration T is 15 μs, constrained by the need for real-time imaging; and the bandwidth is 2-5 MHz, constrained by equipment capabilities. We also assume that the highest blood velocity we can observe is 1.8 m/s. This velocity constraint gives us a stretch factor range of 0.9977-1.0023.

3.2 Blood Flow Estimation Simulations

For our initial simulations, we assume a blood vessel to be located 0.02 m away from the transmitter, of thickness 0.004 m. The blood flow velocity within the vessel is taken to be 1.35 m/s at the endothelium and 1.8 m/s at the center, with a triangular profile. These assumptions model a blood vessel close to the surface of the skin. We assume that this velocity profile is constant, so that there is no acceleration. The blood vessel is modeled as seven discrete targets, each with its own velocity.

The simplest method of velocity estimation is to transmit a single up-chirp, which will be reflected off of each target with some Doppler based on the target's velocity, and correlate the received signal with a Doppler bank of stretched and compressed up-chirps. This cross-correlation is defined as:

$$(f \star g)[n] \stackrel{\text{def}}{=} \sum_{m=-\infty}^{\infty} f^*[m]\, g[m+n] \tag{3.7}$$

Working with discrete signals of finite length, we are able to perform this cross-correlation for each stretched and delayed copy of the transmitted signal. Figure 1 gives the resulting delay-Doppler graph for a hyperbolic up-chirp.

We would have highly localized peaks in the delay-Doppler graph for good delay and Doppler resolution. Instead, we observe that we have good delay resolution but poor Doppler resolution, which produces the lines in Figure 1. The results for the other two chirps do not differ noticeably in their Doppler resolution, with slight differences on the delay scale. The superposed hyperbolic chirp produces a graph similar to Figure 1 in the region of interest, but can produce false peaks outside due to the superposition of the cross-correlations between up- and down-chirps from multiple targets. The linear chirp has better delay resolution but comparable Doppler resolution, as in Figure 2.

We investigate an alternative method of velocity estimation by cross-correlating the received signal from a superposed hyperbolic chirp with an up-chirp and a down-chirp, and observing how the location of peak correlation changes for the two cases. We expect movement of the peak correlation on the delay axis proportional to the velocity of the target. However, we have significant noise for the case

of multiple targets when we perform the correlations, which nonlinearly shifts the peak. Before applying a more sophisticated method to filter out the noise or interpolating to find the approximate peak, we first wish to determine the effects of changing various signal parameters on our Doppler resolution by plotting the wideband ambiguity functions of our chirps. The ambiguity function represents the output of the matched filter and describes the interference caused by the range and Doppler of a target when compared to a reference. We then quantitatively determine the best performance we could theoretically obtain by plotting the Cramér-Rao lower bounds for these signals.

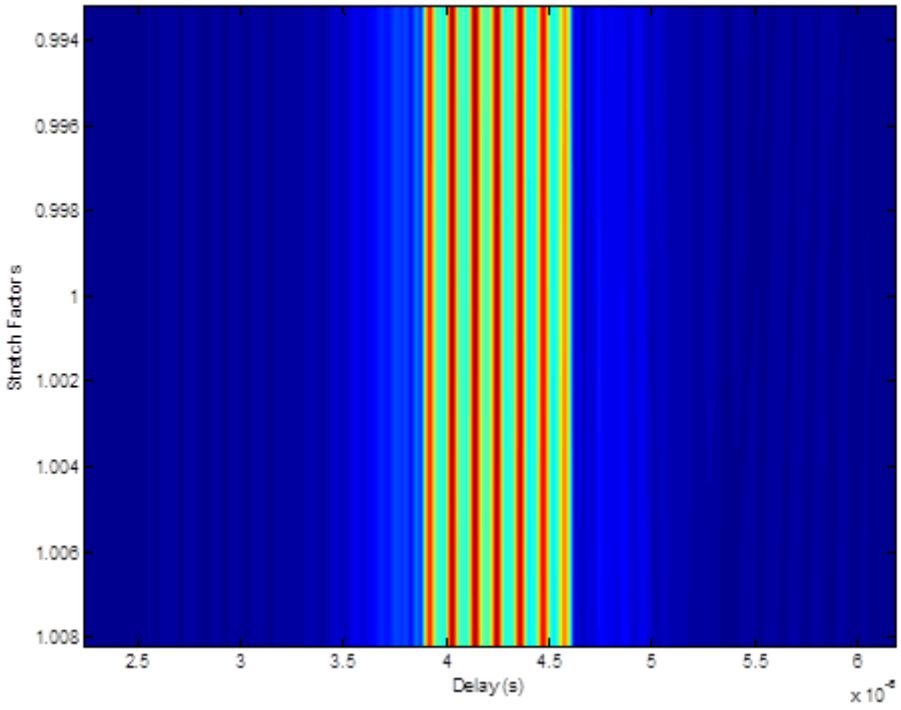

Figure 1: Delay-Doppler Graph Obtained with Filter Bank Approach, Hyperbolic Up-Chirp

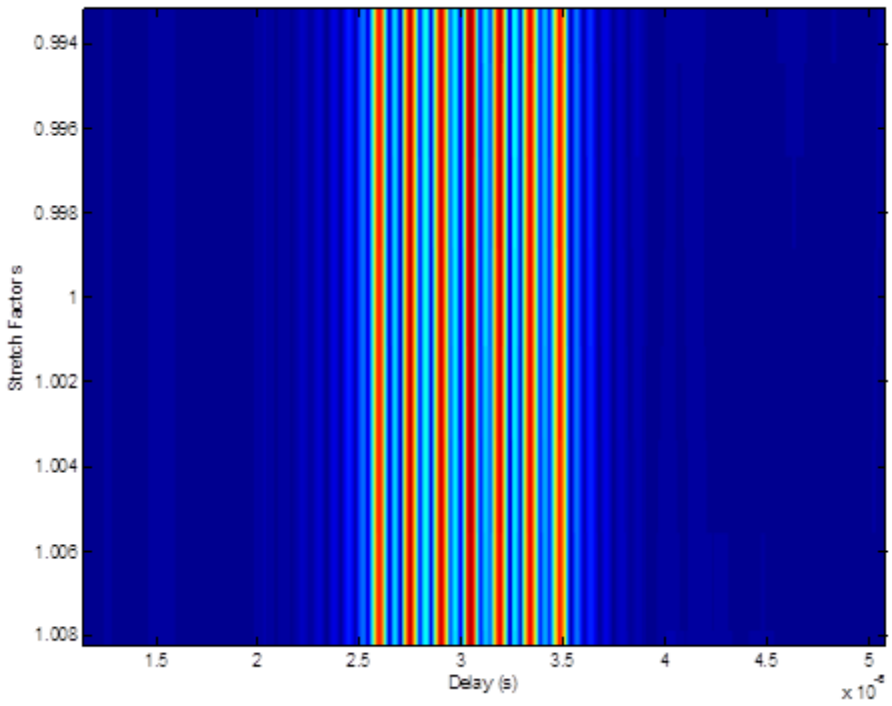

Figure 2: Delay-Doppler Graph Obtained with Filter Bank Approach, Linear Up-Chirp

3.3 True Ambiguity Functions of Chirps

The source of the difficulties we have encountered so far is the poor Doppler resolution we get from our signal duration and bandwidth, which are significantly limited in our model. It is therefore important to determine the best we can achieve with our current parameters; if the constraints are too tight, we may have no choice but to increase our bandwidth or pulse durations. We therefore have to determine the wideband ambiguity functions for our chirps, as a function of delay and Doppler. The method we use is finding the squared difference between a transmitted chirp and its delayed and stretched versions, which is the discrete-time approximation to

$$A(s,d) = \int_{-\infty}^{\infty} \left| g_0(t) - g_0\left(s\left(t - \frac{d}{2}\right) - \frac{d}{2}\right)\right|^2 dt \tag{3.8}$$

where *s* is the stretch factor equal to 1 + Doppler, *d* is delay, and g_0 is our transmitted signal. Our reason for using this wideband expression for the ambiguity function is that our signal experiences non-negligible dilation, in addition to frequency shifts, due to Doppler. Our expression for the received signal is derived from a transmitted signal that experiences *d*/2 delay, stretching *s* due to reflection from a moving target, and a further delay of *d*/2.

We calculate the ambiguity functions of the hyperbolic up-chirp and the superposed hyperbolic chirp, and plot the results as mesh plots in Figures 3 and 4 respectively. Comparing the zero-delay slices for each chirp in Figures 5 and 6, we see that the superposed chirp has slightly better Doppler resolution, but that both chirps have little variation on the Doppler scale.

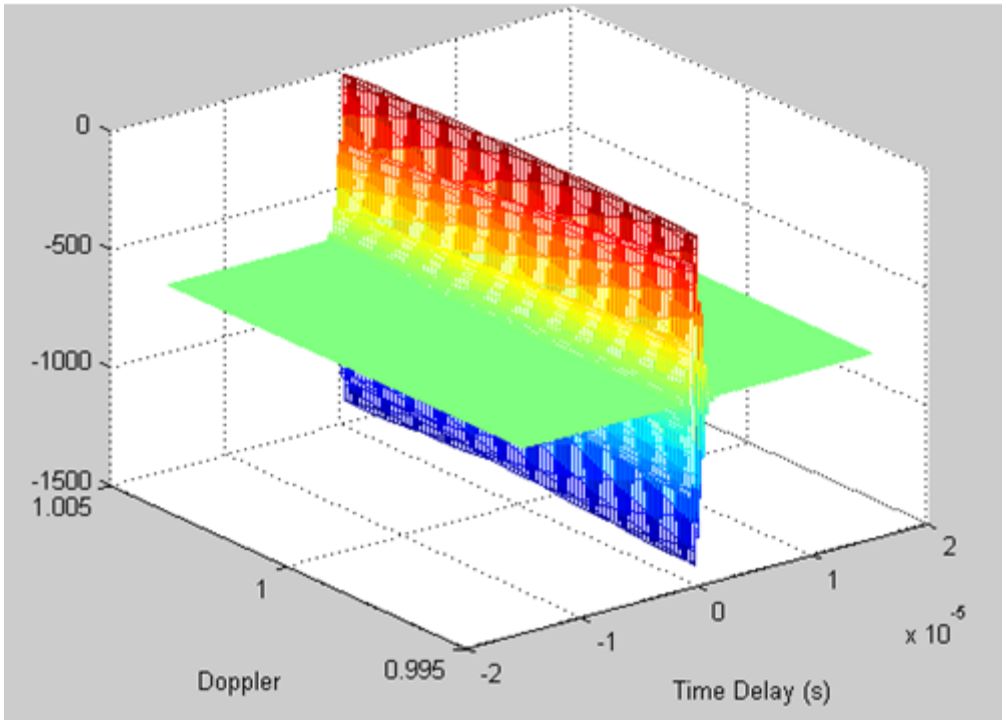

Figure 3: Mesh Plot of Ambiguity Function for Hyperbolic Up-Chirp

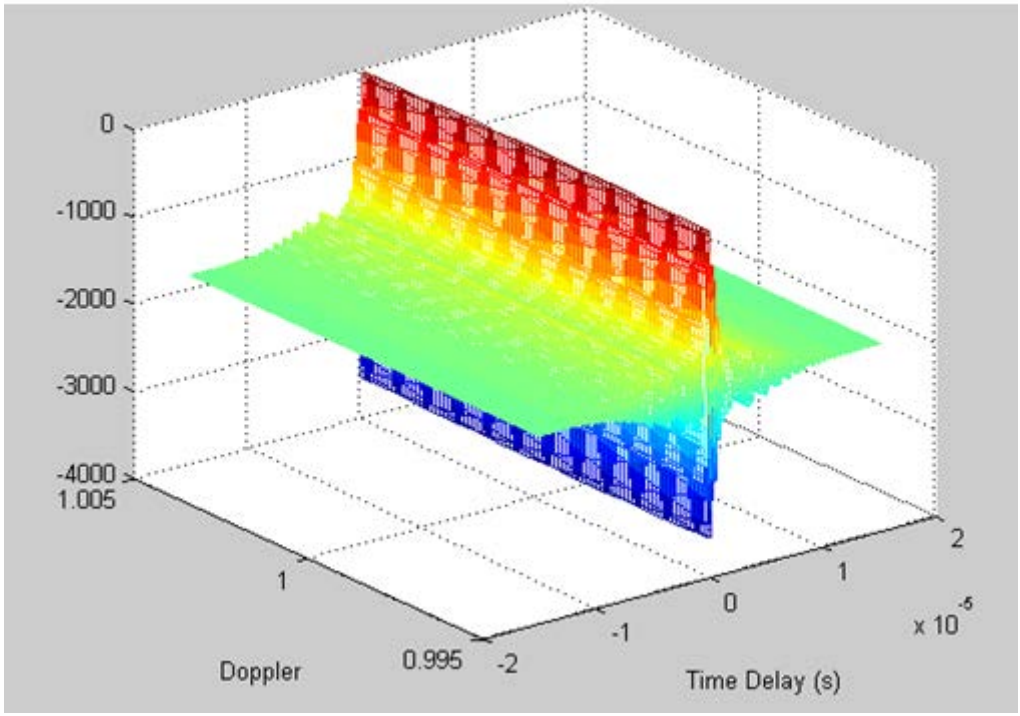

Figure 4: Mesh Plot of Ambiguity Function for Hyperbolic Superposed Chirp

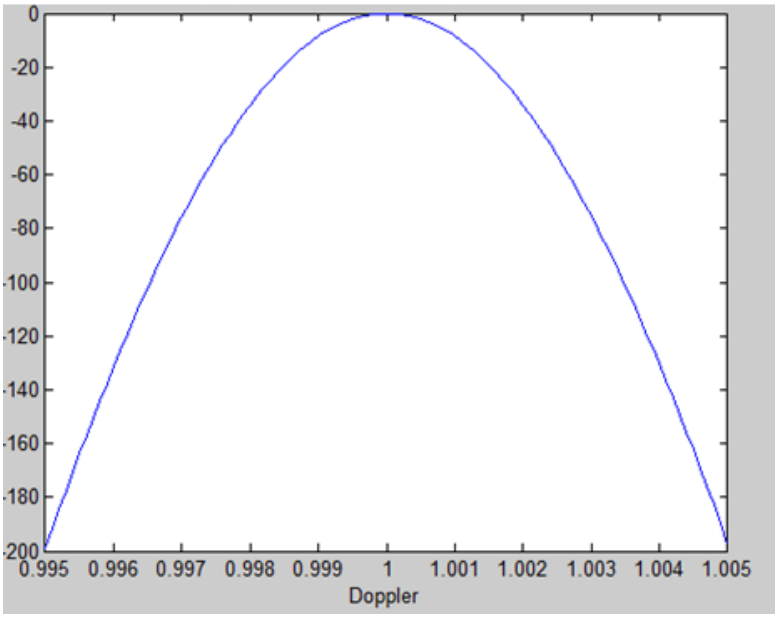

Figure 5: Zero-Delay Slice of Ambiguity Function for Linear Up-Chirp

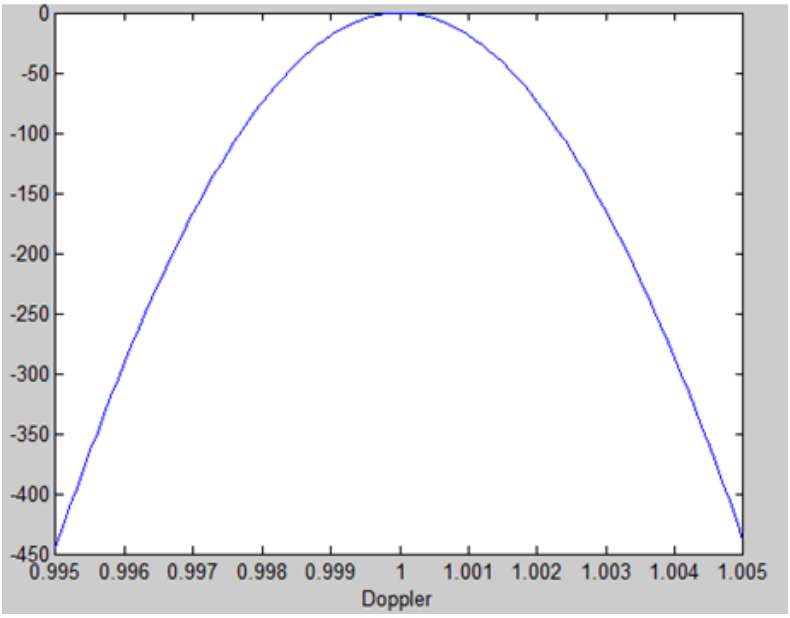

Figure 6: Zero-Delay Slice of Ambiguity Function for Superposed Hyperbolic Chirp

We now wish to observe the effects of increasing pulse duration and bandwidth on spectral resolution. Figures 7 and 8 illustrate the ambiguity functions for a 50 µs-long up-chirp and superposed chirp respectively, for the same bandwidth. Figures 9 and 10 present the zero-delay slices of these two chirps. Figures 11 and 12 give the ambiguity function for an up-chirp and a superposed chirp with three times the bandwidth, corresponding to a frequency range from 2 MHz to 11 MHz. Figures 13 and 14 give the zero-delay slices for the chirps with higher bandwidth.

It is observed that increasing the chirp duration by a factor of 10/3 increases the maximum Doppler variation in the range of interest by more than a factor of 16. Tripling the bandwidth increases Doppler variation only by a factor of 1.5, which is not enough to justify significant resource expenditure in this area. Another important finding is the presence of major peaks in the squared difference plots, situated at small delay and Doppler distances from the original waveform. These give rise to oscillations of the delay locations of correlation peaks over a range of target velocities. The results make it clear that our short pulse duration is the main cause of poor Doppler resolution.

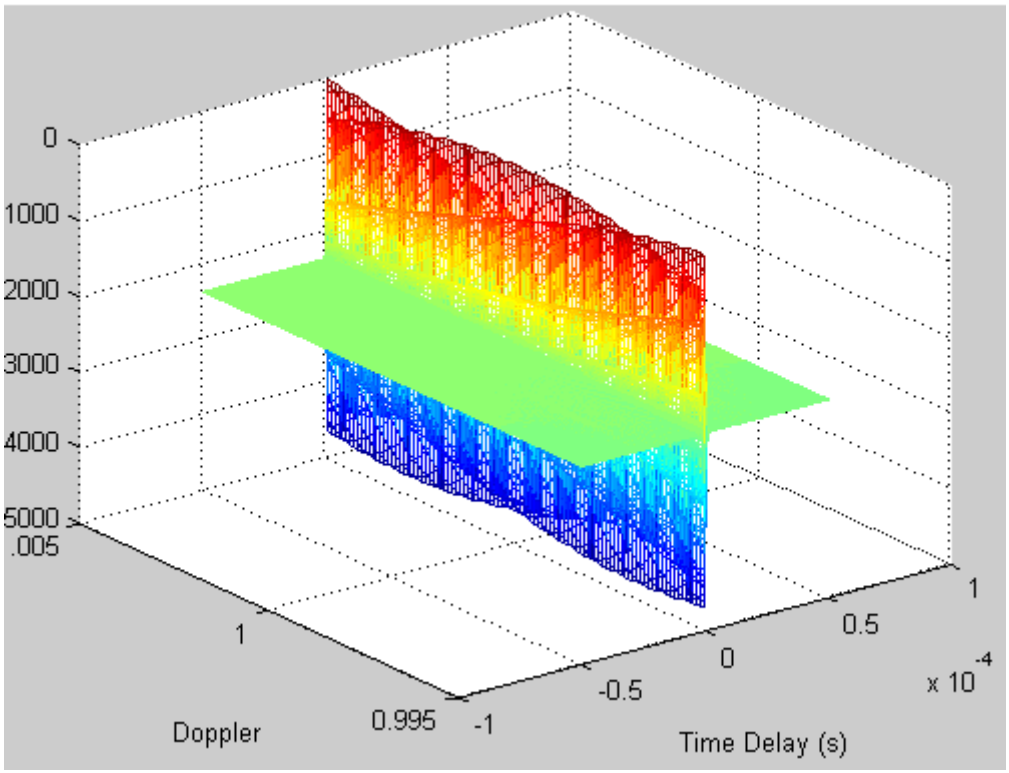

Figure 7: Mesh Plot of Ambiguity Function for Hyperbolic Up-Chirp for Longer Chirp Duration

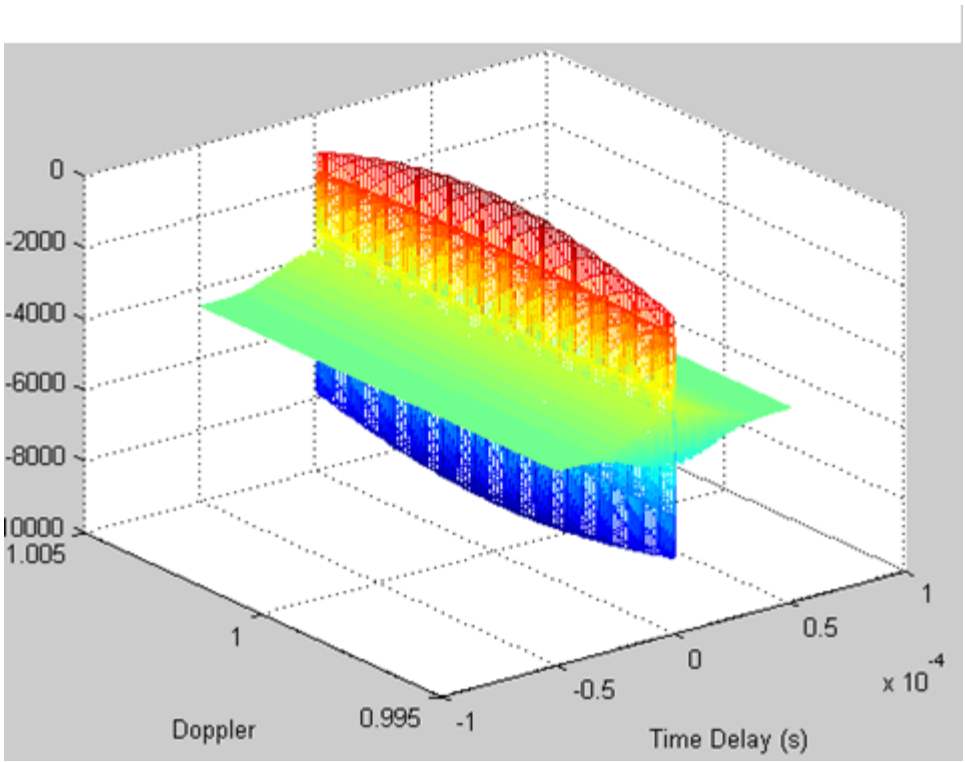

Figure 8: Mesh Plot of Ambiguity Function for Hyperbolic Superposed Chirp for Longer Chirp Duration

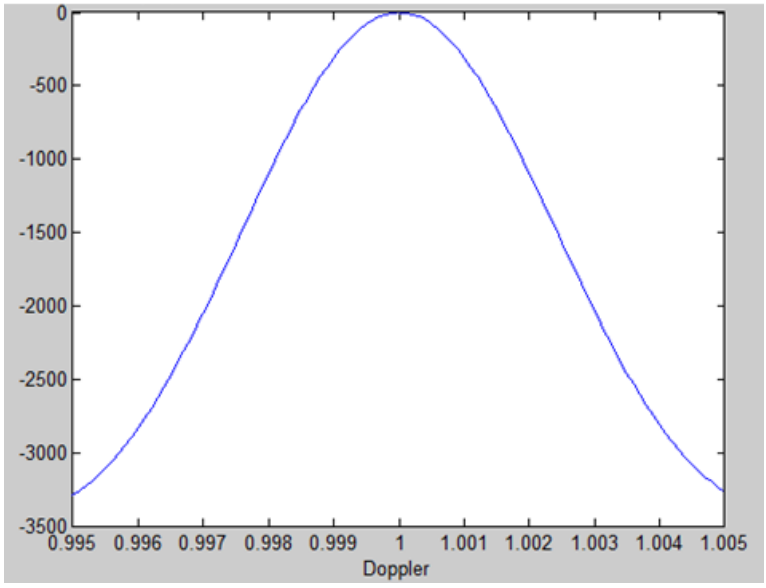

Figure 9: Zero-Delay Slice of Ambiguity Function for 50 µs Linear Up-Chirp

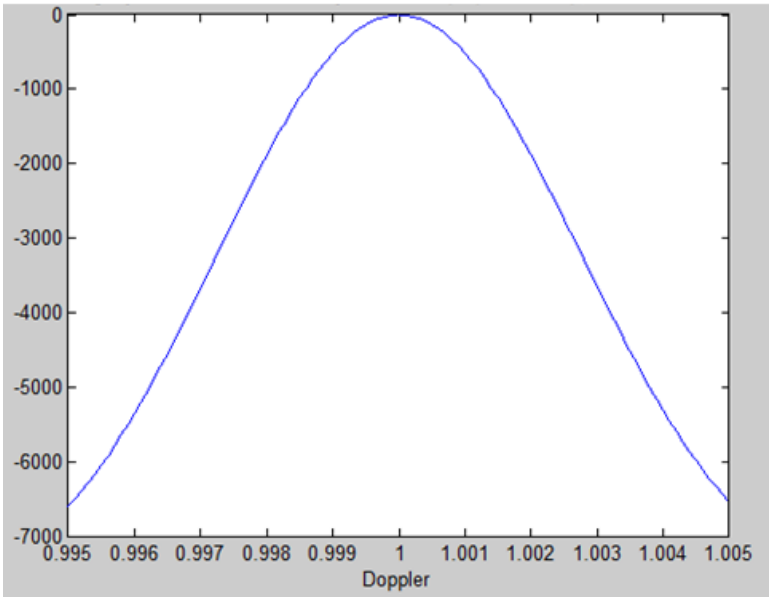

Figure 10: Zero-Delay Slice of Ambiguity Function for 50 µs Superposed Hyperbolic Chirp

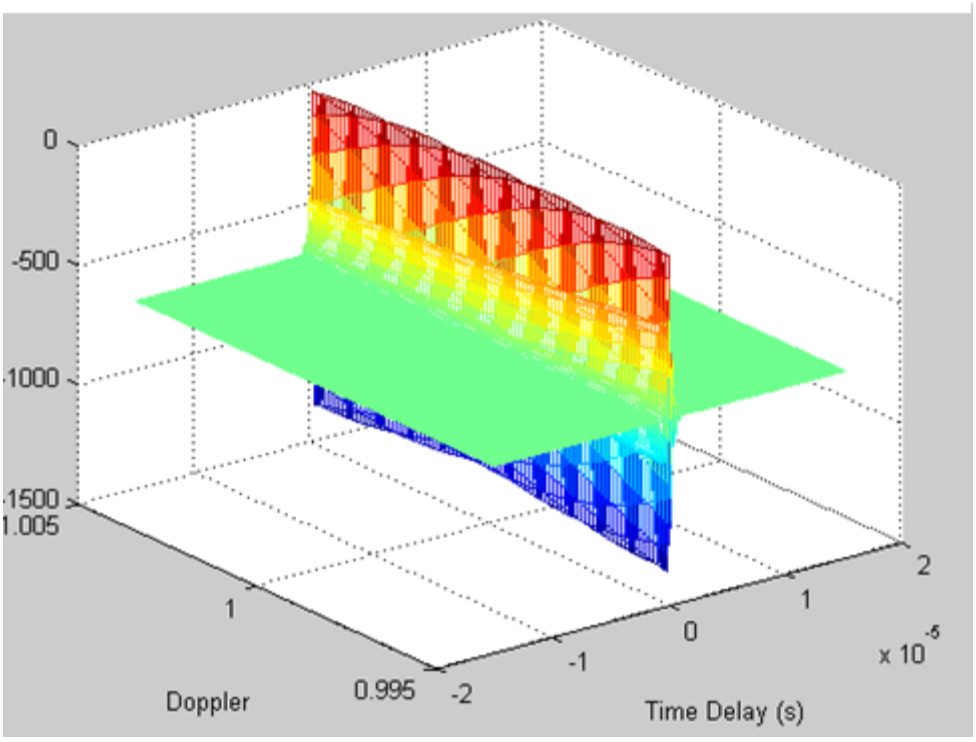

Figure 11: Mesh Plot of Ambiguity Function for Hyperbolic Up-Chirp for Larger Bandwidth

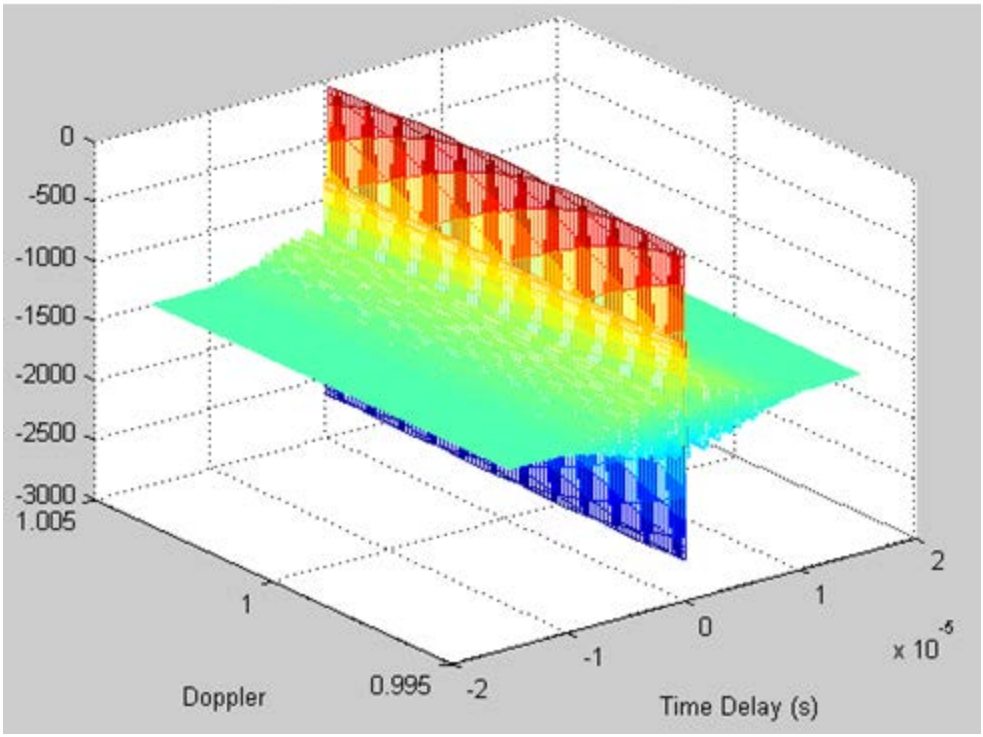

Figure 12: Mesh Plot of Ambiguity Function for Hyperbolic Superposed Chirp for Larger Bandwidth

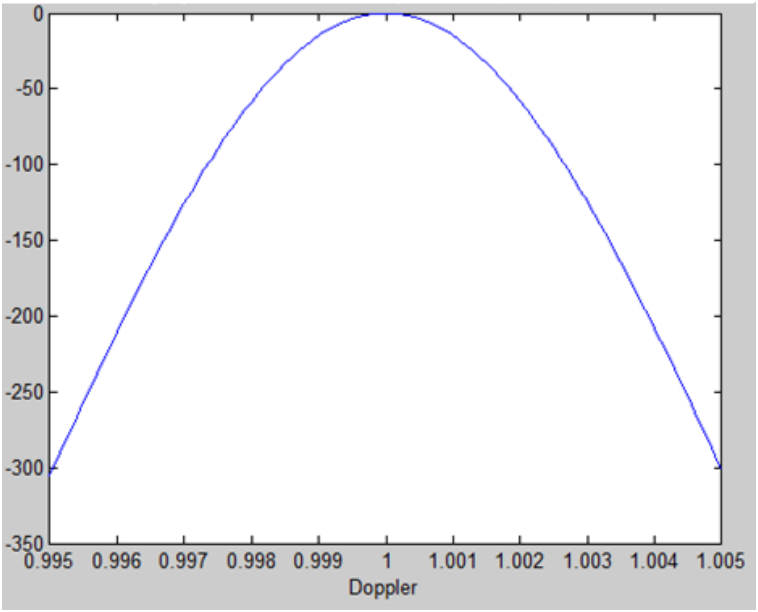

Figure 13: Zero-Delay Slice of Ambiguity Function for Linear Up-Chirp with Larger Bandwidth

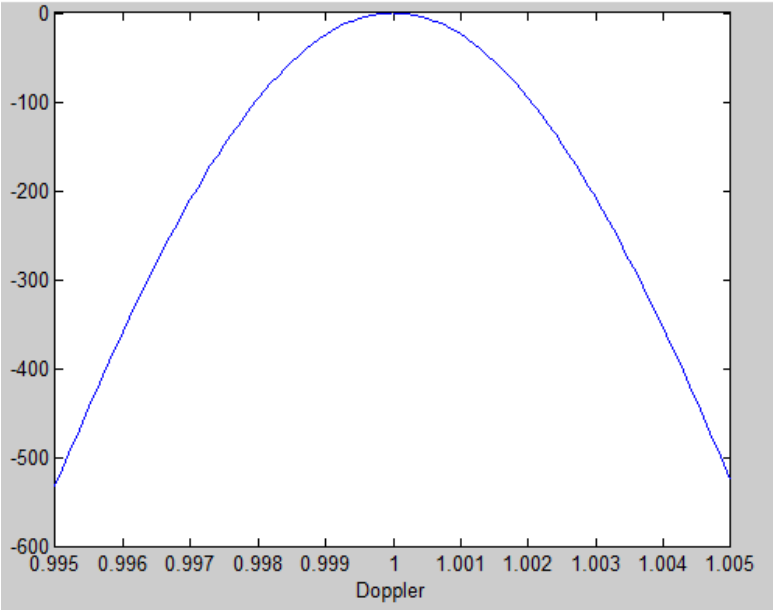

Figure 14: Zero-Delay Slice of Ambiguity Function for Superposed Hyperbolic Chirp with Larger Bandwidth

3.4 Cramér-Rao Lower Bounds

Having determined the limitations imposed by the problem constraints, we now need to know the best-case theoretical resolution we could obtain for a given delay, Doppler and SNR. In the presence of a single target at Doppler stretch s_0 and delay d_0, we want to find lower bounds on the variance of an estimator of its delay and Doppler when the received signal is buried in Gaussian noise. Sections 3 and 15 of *Fundamentals of Statistical Signal Processing: Estimation Theory* by Steven M. Kay [6] and Chapter 8 of *Optimum Array Processing* by Harry L. Van Trees [7] have been consulted to formulate the Cramér-Rao lower bound (CRLB) for our problem. While it is possible to derive the CRLB for each application as a closed-form linear algebraic expression, as Van Trees does, we use the more general approach of calculating the entries of a 2x2 Fisher information matrix and inverting it to obtain our lower bounds in delay and Doppler on the diagonal entries. For a given signal $u(t;s_0,d_0)$, the Fisher information matrix F is given by

$$F = \frac{A^2}{2\sigma^2}\begin{bmatrix} \int \left|\frac{\partial}{\partial s}u(t;s_0,d_0)\right|^2 dt & \int \left(\frac{\partial}{\partial s}u^*(t;s_0,d_0)\right)\left(\frac{\partial}{\partial d}u(t;s_0,d_0)\right) dt \\ \int \left(\frac{\partial}{\partial s}u(t;s_0,d_0)\right)\left(\frac{\partial}{\partial d}u^*(t;s_0,d_0)\right) dt & \int \left|\frac{\partial}{\partial d}u(t;s_0,d_0)\right|^2 dt \end{bmatrix} \quad (3.9)$$

where A is an amplitude coefficient and σ^2 is the variance of complex Gaussian noise. For complex Gaussian noise, SNR is given by A^2/σ^2 [6]. Since it is the ratio of the amplitude to variance that we are

interested in, we can take $\sigma^2 = 1$ without loss of generality, so for a given SNR we can calculate A as $\sqrt{SNR}$.

To calculate the CRLB for our chirps, we first write a closed form expression for the received chirp which has been delayed by d and Doppler-shifted by s. We note that the received chirp's amplitude is scaled by s^2 as a consequence of energy conservation. We can also make the approximation that

$$u\left(s\left(t-\frac{d}{2}\right)-\frac{d}{2}\right) \approx u(st-d) \tag{3.10}$$

for the range of delays and Dopplers that we are interested in, because s is close to 1. This assumption greatly simplifies our calculations without making a noticeable difference in our results. As an example, the closed-form expression for our simple hyperbolic chirp is given by

$$C(t)_{hyper} = s^2 e^{j(2\pi / k_0)\log(1+k_0 f_0(st-d))} \tag{3.11}$$

Having formulated a closed-form expression for the chirp, we write it in MATLAB as a symbolic expression in s, t and d, and take its derivatives with respect to s and d to come up with closed-form expressions of the entries of the Fisher information matrix. For example, for the linear up-chirp, we obtain derivatives:

$$\frac{\partial u}{\partial s} = \frac{(2s)}{e^{2\pi j(2000000d-2000000st+(d-st)^2/100}} + \frac{\left(2\pi j s^2(2000000t+t(d-st)/50)\right)}{e^{2\pi j(2000000d-2000000st+(d-st)^2/100}} \tag{3.12}$$

$$\frac{\partial u}{\partial d} = \frac{-\left(2\pi j s^2\left(\frac{d-st}{50}+2000000\right)\right)}{e^{2\pi j(2000000d-2000000st+(d-st)^2/100}} \tag{3.13}$$

After we have obtained these derivatives, we can substitute the results into (3.9) to obtain the entries of the Fisher information matrix. In a separate routine, we substitute numerical values s_0 and d_0 for s and d since we want to obtain the CRLB for a given delay and Doppler, and write the entries as symbolic expressions of t only. We perform numerical integrations of the matrix entries with respect to t for $[d_0, s_0T + d_0]$, which is the time range in which we encounter the chirp. Having obtained numerical results for each entry of F, we invert the matrix. The CRLB in Doppler is given by the (1,1) entry of the resulting matrix, and the CRLB in delay is given by the (2,2) entry. It is the bound for Doppler that we are mainly interested in, and we plot this for a range of SNR on a logarithmic scale for the y-axis.

Figure 15 gives the SNR variation of the CRLB in Doppler estimate for a 15 µs linear chirp with *s* = 1 and *d* = 20 µs, which are reasonable parameters for our problem. Figures 16 and 17 plot the CRLB for hyperbolic and superposed hyperbolic chirps with the same parameters. Since the superposed hyperbolic chirp is the sum of two hyperbolic chirps, we scale its amplitude by $1/\sqrt{\mathbf{2}}$ for a fair comparison.

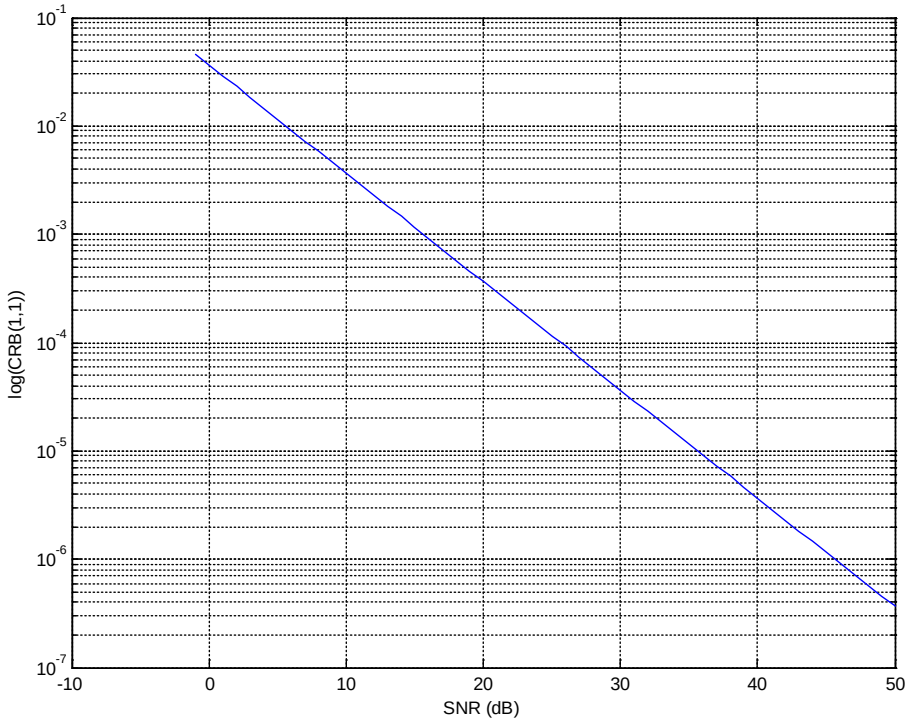

Figure 15: SNR Variation of Cramer-Rao Bound in Doppler Estimate for s = 1, d = 20µs, 15 µs Linear Chirp

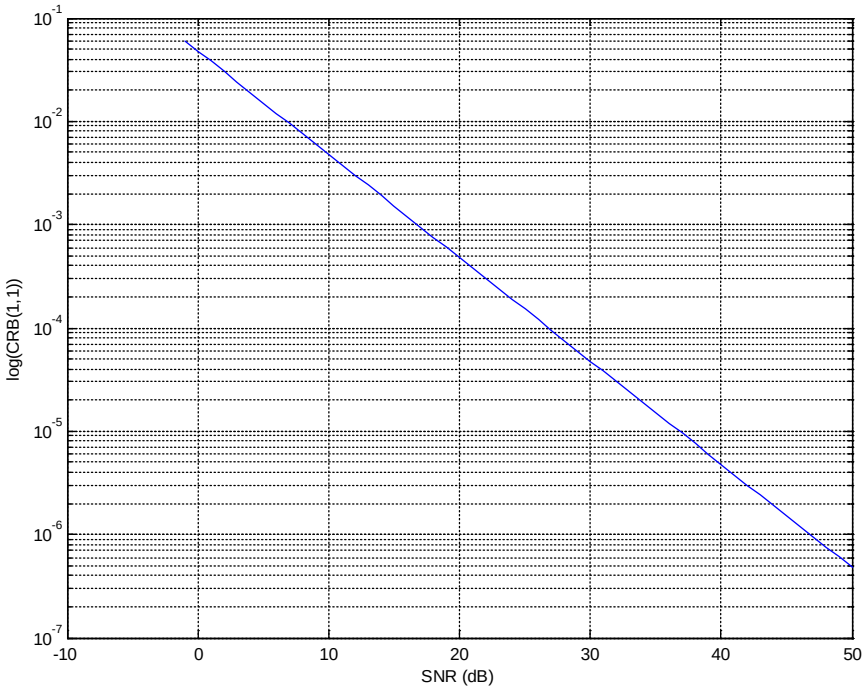

Figure 16: SNR Variation of Cramer-Rao Bound in Doppler Estimate for s = 1, d = 20μs, 15 μs Hyperbolic Chirp

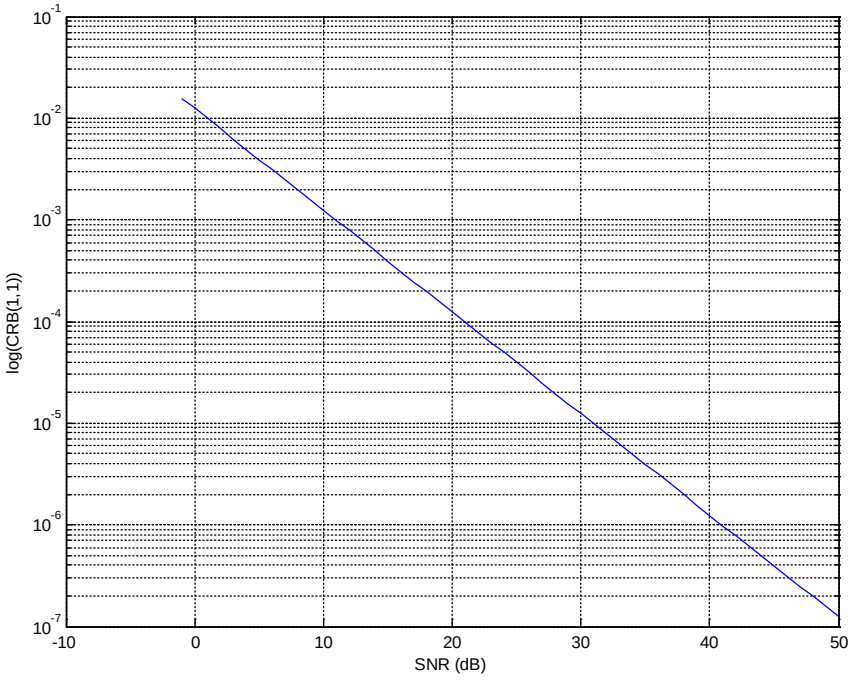

Figure 17: SNR Variation of Cramer-Rao Bound in Doppler Estimate for s = 1, d = 20μs, 15 μs Superposed Hyperbolic Chirp

The CRLB plots yield numerical results that confirm our previous observations. The linear chirp and hyperbolic chirp have Cramér-Rao lower bounds that are close to each other; we had seen previously that the ambiguity functions of these chirps have similar profiles for short pulse durations. The linear chirp has a slightly lower bound on the logarithmic plot. The superposed hyperbolic chirp has the lowest CRLB in Doppler, and is our best candidate for the transmitted signal. The range of Doppler variation we get for blood velocity is s = 0.9978-1.0022, corresponding to a maximum velocity of 1.8 m/s in any direction. We would like to observe Doppler on the order of 10^{-4} if possible for accurate measurement of transient phenomena. We need around 25 dB of SNR for the linear and hyperbolic chirps and around 21 dB for the superposed hyperbolic chirps to achieve this resolution, based on the CRLB plots we have obtained. This range of SNR is easily attained for ultrasound systems using chirps. We must note that our chirp expression does not include the frequency-dependent attenuation factor that results from the nonlinear characteristics of the human body. In the frequency domain, the amplitude attenuation transfer function for a plane wave propagating through a tissue is given by:

$$|H(f;z)| = e^{-(\beta_0 z + \beta_1 f z)} \tag{3.14}$$

where z is depth in tissue, f is frequency, β_0 is the frequency-independent attenuation, and β_1 is the frequency-dependent term [3]. The addition of this factor would drive the CRLB higher, because it would make the entries of the Fisher information matrix smaller and thus result in a higher CRLB when the matrix is inverted. The incorporation of this term into our chirp expression and the calculation of the CRLB for the case of attenuation is the first step in our future research.

4. Conclusion

This thesis addressed the problem of Doppler-based ultrasonic blood velocity estimation. The preliminary literature survey emphasized the great difficulty of obtaining good Doppler estimates for blood flow; we hoped that recent advances in electrical engineering could be used to solve this problem. The first step in our research was to simulate the basic case of a simple chirp incident on a blood vessel, undergoing delay and Doppler shift. We confirmed that there was indeed very little Doppler information to be extracted from the received waveform, and that our candidate methods involving the use of superposed chirps needed further refinement. Before proceeding with new approaches to the problem, we decided to conduct a more thorough feasibility study, focusing on the limitations of the chirps we use. We plotted the true ambiguity functions of each chirp for different durations and bandwidths, and observed that the 15 μs constraint was the limiting factor for Doppler resolution; conversely, we confirmed that we did not need additional bandwidth. Finally, we plotted the Cramér-Rao lower bounds in Doppler of each chirp to determine the SNR needed to make Doppler-based methods feasible. We determined that for the case of a delayed and Doppler-shifted linear or hyperbolic chirp, we needed at least 25 dB of SNR to obtain the Doppler resolution required by the blood flow problem; for a superposed hyperbolic chirp, 21 dB of SNR is sufficient. This was an encouraging result, since SNR greater than 20 dB is easily obtained for chirp-based ultrasound methods.

There is a great deal of research still to be done for a full study of Doppler-based methods. Our received chirp model has to be refined to include attenuation due to the acoustic properties of the human body, and a new Cramér-Rao lower bound has to be calculated. This will drive up the required SNR for accurate Doppler measurement. More advanced signal processing methods will be applied to improve our results for superposed hyperbolic chirps; and the results we obtain for a range of SNR will be plotted against the Cramér-Rao lower bound to determine their effectiveness. If we are successful in accurately determining Doppler information from blood flow, we can apply the techniques we have developed to a wide variety of applications.

My undergraduate research has been an excellent educational experience. I have built a toolbox of key signal processing techniques – modeling delay and Doppler, plotting ambiguity functions, and determining the Cramér-Rao lower bound – which I will use throughout my career as an electrical engineer. Undertaking a risky research project on my own has allowed me to experience every step of the research cycle. I will be continuing my research on blood velocity as a graduate student at UIUC.

References

[1] K.K Shung. *Diagnostic Ultrasound: Imaging and Blood Flow Measurements*, Taylor and Francis Group, LLC, 2006.

[2] D.H. Evans, J.A. Jensen and M.B. Nielsen, "Ultrasonic Color Doppler Imaging," Interface Focus, 2011.

[3] J. A. Jensen, *Estimation of Blood Velocities Using Ultrasound*, Cambridge University Press, New York, 1996.

[4] C. Kasai, K. Namekawa, A. Koyano and R. Omoto, "Real-Time Two-Dimensional Blood Flow Imaging Using an Autocorrelation Technique," *IEEE Trans. Sonics Ultrason*., vol. SU-32, May 1985.

[5] J. Yang and T.K. Sarkar, "Acceleration-invariance of hyperbolic frequency modulated pulse compression," *Digital Signal Process*, Volume 18, Issue 2, March 2008, pp. 228–235.

[6] S. Kay, "Cramer-Rao Lower Bound," in *Fundamentals of Statistical Signal Processing: Estimation Theory, Vol. I*. A. V. Oppenheim, Prentice-Hall, Englewood Cliffs, NJ, 1988.

[7] H.L Van Trees. *Detection, Estimation and Modulation Theory, Optimum Array Processing*, John Wiley & Sons, 2004.